molecular pharmaceutics

Article

pubs.acs.org/molecularpharmaceutics

Controlled Protein Delivery from Electrospun Non-Wovens: Novel Combination of Protein Crystals and a Biodegradable Release Matrix

Sebastian Puhl,[†] Linhao Li,[†,‡] Lorenz Meinel,[†] and Oliver Germershaus*[,†]

[†]Institute for Pharmacy and Food Chemistry, University of Wuerzburg, Am Hubland, DE-97074 Wuerzburg, Germany

[‡]Key Laboratory of Biorheological Science and Technology, Ministry of Education, College of Bioengineering, Chongqing University, Chongqing 400030, P. R. China

Supporting Information

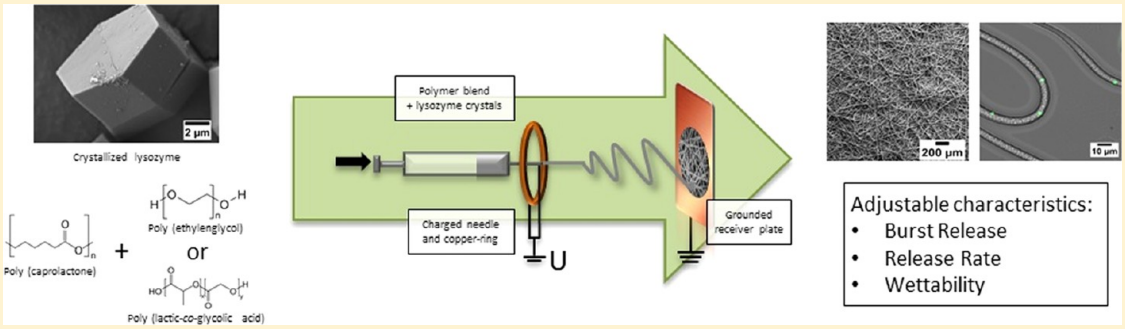

ABSTRACT: Poly-ε-caprolactone (PCL) is an excellent polymer for electrospinning and matrix-controlled drug delivery combining optimal processability and good biocompatibility. Electrospinning of proteins has been shown to be challenging via the use of organic solvents, frequently resulting in protein unfolding or aggregation. Encapsulation of protein crystals represents an attractive but largely unexplored alternative to established protein encapsulation techniques because of increased thermodynamic stability and improved solvent resistance of the crystalline state. We herein explore the electrospinning of protein crystal suspensions and establish basic design principles for this novel type of protein delivery system. PCL was deployed as a matrix, and lysozyme was used as a crystallizing model protein. By rational combination of lysozyme crystals 0.7 or 2.1 µm in diameter and a PCL fiber diameter between 1.6 and 10 µm, release within the first 24 h could be varied between approximately 10 and 100%. Lysozyme loading of PCL microfibers between 0.5 and 5% was achieved without affecting processability. While relative release was unaffected by loading percentage, the amount of lysozyme released could be tailored. PCL was blended with poly(ethylene glycol) and poly(lactic-*co*-glycolic acid) to further modify the release rate. Under optimized conditions, an almost constant lysozyme release over 11 weeks was achieved.

KEYWORDS: *electrospinning, protein delivery, poly(caprolactone), protein crystal, poly(lactic-glycolic acid)*

1. INTRODUCTION

The first report of electrospinning dates back to the 1930s.[1,2] Besides good processability and high versatility with regard to attainable structures of the products, electrospun non-wovens are quite suitable as controlled release matrices for drug delivery. With the increasing availability of biocompatible polymers being suitable for electrospinning, controlled drug release from non-woven scaffolds has received an increasing amount of attention. Potential applications of non-wovens range from transdermal delivery and wound dressing to tissue engineering after surgical intervention.[3]

Poly-ε-caprolactone (PCL) is a biocompatible and biodegradable polymer with proven suitability for controlled drug delivery applications.[4] The solubility in various organic solvents as well as its ability to form fibers under mechanical stress renders PCL an ideal candidate for electrospinning.[5] PCL biodegradation *in vivo* is slow and primarily driven by enzymatic degradation. *In vitro*, its structure remains intact over months.[6] Poly(lactic-*co*-glycolic acid) (PLGA) represents a well-established polymer for drug delivery with a degradation rate that is higher than that of PCL but is hampered by significant shrinkage of its non-wovens.[7] The combination of PCL and PLGA leads to easily processable polymer blends, mechanically stable non-wovens, and allows the fine-tuning of release properties.[8] However, PCL and PLGA both are rather hydrophobic polymers, and poor wettability frequently is a challenge for efficient drug release.[9] Therefore, hydrophilic polymers, such as poly(ethylene glycol) (PEG) or poly(ethyleneimine), have been used to improve wettability as well as to induce pore formation and resulted in successful efforts to improve drug release.[9−11]

Received: February 3, 2014
Revised: April 28, 2014
Accepted: May 27, 2014
Published: May 27, 2014

dx.doi.org/10.1021/mp5001026 | *Mol. Pharmaceutics* 2014, 11, 2372−2380

The controlled release of proteins is a long-standing challenge to formulation scientists because of the complex structure, multiple degradation pathways, and resulting stability issues. Unfortunately, electrospinning often relies on the use of organic solvents that may detrimentally affect protein integrity and thus their biological activity. Electrospinning of water in oil emulsions and generation of lipophilic complexes of hydrophilic proteins are common solutions.[9,10] Nevertheless, proteins are still prone to interactions with the solvent or the solvent−water interface, rendering them susceptible to denaturation. Considering these challenges, the aim of this work was to establish alternative strategies for the encapsulation of proteins.

Compared to the amorphous state, crystals are characterized by higher thermodynamic stability and a reduced solvent-exposed surface area, rendering protein crystals potentially more suitable for direct processing in organic solvents.[12−14] As an example, α-amylase was shown to withstand treatment with organic solvents after crystallization.[15] In addition, crystals represent the most concentrated form of a protein, therefore allowing high drug loading.[12] Finally, crystal dissolution can be controlled in many ways, e.g., by modifying crystal size, crystal morphology, excipients, and dissolution media.[12,16] Because of these properties, the encapsulation of protein crystals into polymeric matrices by electrospinning may represent an alternative approach alleviating several of the problems encountered during generation of protein drug delivery systems.

Lysozyme was selected as a model protein on the basis of its well-established crystallization conditions, allowing the generation of crystals with a controlled size and morphology.[17] Moreover, lysozyme is well-established for wound treatment.[18−20]

Lysozyme crystals with a well-controlled, narrow size distribution were prepared, and the impact of PCL fiber diameter and size of incorporated protein crystals on drug release was studied. Furthermore, lysozyme loading was varied to identify the effect on processability and release. We then used PCL/PEG and PCL/PLGA blends to improve the hydrophilicity, microporosity, and degradability of the fibers to modify drug release kinetics.

2. EXPERIMENTAL SECTION

2.1. Materials. Chicken egg white lysozyme (∼70000 units/mg), PCL (M_w = 70000−90000), *Micrococcus lysodeikticus*, polysorbate 80 (PS80), fluorescein isothiocyanate (FITC), and tetrafluoroacetic acid [high-performance liquid chromatography (HPLC) grade] were purchased from Sigma-Aldrich (Munich, Germany). Poly(D,L-lactide-*co*-glycolide) 50:50 (Resomer RG 502H, M_w = 7000−17000, free acid) was a gift from Evonik Industries (Essen, Germany). Poly(ethylene glycol) 3000 was obtained from MERCK Schuckardt (Hohenbrunn, Germany). The bicinchoninic acid (BCA) assay kit was purchased from Thermo Scientific (Rockford, IL). Acetonitrile (gradient grade) was purchased from VWR Prolabo (Fontenay-sous-Bois, France). Chloroform, ethanol, sodium phosphate, sodium hydroxide, sodium chloride, sodium azide, and acetic acid were of analytical grade.

2.2. Lysozyme Crystallization and Crystal Size Determination. Lysozyme crystallization was performed according to the method of Falkner et al. with modifications.[17] Lysozyme was dissolved in 10 mL of sodium acetate buffer (pH 3.5) at a concentration of 8.0 mg mL^{-1}. Twenty milliliters of precipitation buffer consisting of 20% sodium chloride, 10% PEG 3000, and 500 mM sodium acetate (pH 3.5) at −4 or 8 °C was poured quickly into the lysozyme solution and the mixture stirred at 500 rpm. Crystal formation took place within seconds. After being washed twice with an ethanol/chloroform mixture (3:10 volume ratio), crystals were dried under a mild vacuum. Particle size distributions of particles above approximately 1 μm were determined by laser diffraction analysis (LS 230, Beckman Coulter, Brea, CA) and below approximately 1 μm by dynamic light scattering (DelsaNano HC, Beckman Coulter).

2.3. FITC Labeling of Lysozyme. Lysozyme was dissolved in 0.1 M carbonate buffer (pH 9.0) at a concentration of 2.0 mg mL^{-1}. FITC (1.0 mg mL^{-1}, dissolved in DMSO) was added at a volume ratio of 1:12.5 to the lysozyme solution and the mixture stirred for 6 h at room temperature. Subsequently, the solution was dialyzed (Spectra/Por dialysis membrane, cutoff of 6−8 kDa, Spectrum Laboratories, Rancho Dominguez, CA) against 5 L of deionized water for 2 h and lyophilized. The average molar degree of modification was 1.47 mol (mol of FITC)$^{-1}$ per lysozyme. Labeled crystals were produced using a 1:30 labeled:unlabeled lysozyme molar ratio according to the procedure described above.

2.4. PCL Electrospinning. Electrospinning was performed with a dc power supply HCP 140-350000 instrument from FuG Elektronik (Rosenheim, Germany) and a syringe pump (type 540200, TSE Systems, Bad Homburg, Germany). PCL fibers were produced by electrospinning onto a static receiver plate using a focusing ring 20 cm in diameter using a setup similar to that described previously.[21] Protein crystals were suspended in ethanol at a concentration of 3.0 mg mL^{-1}. After homogenization in an ultrasonic bath (Branson 3200, Bransonic, Danbury, CT) for 20 s, chloroform and the respective polymers were added. Ethanol and chloroform were mixed in a volume ratio of 1:6. Using this procedure, stable protein crystal suspensions in a concentrated PCL solution, suitable for electrospinning, were obtained. Suspensions were transferred into a syringe with an attached metal spinneret (22 gauge). A copper ring with a 20 cm diameter was electrically charged like the metal spinneret and placed in a vertical plane around it. The electrospinning conditions, composition of the polymer solution, and lysozyme crystal size were varied, resulting in different combinations of crystal size and fiber diameter (Table 1). For each sample, 1 mL of a polymer suspension was electrospun, resulting in round non-wovens with almost identical diameters. The loading of the non-wovens was calculated to be 0.2% m/m. Pure PCL non-wovens with lysozyme loadings of 0.5, 1.0, 2.5, and 5.0% were produced using 2.1 μm lysozyme crystals with minor adjustments. A

Table 1. Electrospinning Conditions and Resulting Average Fiber Diameters of Pure PCL Fibers

crystal size (μm)	PCL (% m/V)	flow rate (mL h^{-1})	collector distance (cm)	voltage (kV)	fiber diameter ± SD (μm)
2.1	14	1	20	25	1.7 ± 0.5
0.7	14	1	20	25	1.6 ± 0.4
2.1	14	5	25	25	3.9 ± 0.5
0.7	14	5	25	25	3.5 ± 0.8
2.1	18	10	25	25	5.3 ± 0.7
0.7	18	10	25	25	5.2 ± 0.5
2.1	25	15	35	25	10.1 ± 0.8
0.7	25	15	35	25	10.3 ± 1.0

dx.doi.org/10.1021/mp5001026 | Mol. Pharmaceutics 2014, 11, 2372−2380

Table 2. Electrospinning Conditions and Resulting Average Fiber Diameters of PCL/PEG Blends

PEG content (% m/m)	crystal size (μm)	PCL (% m/V)	flow rate (mL h^{-1})	collector distance (cm)	voltage (kV)	fiber diameter ± SD (μm)
2	2.1	25	15	40	27	6.8 ± 1.1
5						6.9 ± 0.9
10						5.8 ± 0.9[a]
20						5.6 ± 1.1[a]

[a]Fiber diameters are statistically significantly smaller than those of a 2% PCL/PEG blend ($p < 0.001$).

Table 3. Electrospinning Conditions and Resulting Average Fiber Diameters of PCL/PLGA Blends

PLGA content (% m/m)	crystal size (μm)	PCL (% m/V)	flow rate (mL h^{-1})	collector distance (cm)	voltage (kV)	fiber diameter ± SD (μm)
2	2.1	25	15	40	27	9.9 ± 3.4
10						8.2 ± 4.4[a]

[a]Fiber diameters are statistically significantly smaller than those of a 2% PCL/PLGA blend ($p < 0.024$).

solution of 18% m/V PCL was electrospun with a flow rate of 10 mL h^{-1}. The collector was placed at a distance of 35 cm, and the voltage was set to 27 kV. The resulting fiber diameter was 7.11 ± 3.01 μm. Furthermore, different amounts of PEG or PLGA were admixed to the PCL/crystal suspension and electrospun in a similar fashion (Tables 2 and 3). Concentrations of admixed PEG or PLGA were calculated relative to total dry polymer mass (% m/m). All experiments were performed in triplicate, and the data represent averages ± the standard deviation (SD).

2.5. *In Vitro* Release. The generated non-wovens were dried in vacuum overnight and weighed. Afterward, the entire non-woven (approximately 150−300 mg) was cut into smaller pieces and incubated in 3.0 mL of PBS (pH 7.4) with 0.1% sodium azide at 37 °C. At each time point, 200 μL of the release medium was withdrawn and replaced by the same volume of buffer. To minimize the impact of the variable wettability of scaffolds and to delineate the effect of fiber diameter and crystal size, polysorbate 80 was added to the release medium during release from pure PCL non-wovens. In contrast, the medium used during release from PCL/PEG and PCL/PLGA blends was without PS 80. The lysozyme concentration was measured by RP-HPLC (LaChrom Ultra with L-2400 UV dectector, VWR Hitachi and RP18 Licrosphere 100 column, Merck, Darmstadt, Germany) at 220 nm (λ) with a water/TFA to acetonitrile gradient (Table S1 of the Supporting Information), yielding a limit of quantification of 2.56 μg mL^{-1}. The BCA assay (Pierce BCA assay kit, Thermo Scientific) was used for lysozyme quantification in the case of PCL/PEG and PCL scaffolds where release medium without polysorbate 80 was used, and the limit of quantification was 1.20 μg mL^{-1}. Fifty microliters of sample was mixed with 200 μL of the BCA reagent solution. After incubation at 60 °C for 30 min, the absorbance was determined at a wavelength (λ) of 562 nm (Spectra max 250, Molecular Devices, Sunnyvale, CA).

2.6. Relative Bioactivity of Lysozyme. The relative bioactivity of lysozyme was determined as described previously.[22] Briefly, the *Micrococcus lysodeikticus* cell wall preparation was suspended in 1.0 mL of 0.1 M KH_2PO_4 (pH 6.2) at a concentration of 200 mg L^{-1}, and 33.3 μL of the sample solution was added. After the sample had been stirred for 5 s, the decline in absorbance measured at 570 nm was recorded for 2 min (Genesys 10S, Thermo Scientific). The relative biological activity of lysozyme was determined in reference to a calibration curve constructed using fresh lysozyme and setting its bioactivity to 100%. The slope of the decline was proportional to the lysozyme activity, and the limit of quantification was 0.96 μg mL^{-1} lysozyme.

2.7. Morphology and Fiber Diameter. Scanning electron microscopy (SEM) images were recorded using a JSM-7500F field emission scanning electron microscope (Jeol, Tokyo, Japan) with an acceleration voltage of 5 kV. The fiber diameter was determined using ImageJ (National Institutes of Health, Bethesda, MD). For each preparation, 60 individual fiber diameters were measured manually perpendicular to the fiber surface. For all preparations, samples of non-wovens were drawn regularly during release studies. Samples were washed with purified water, dried under vacuum overnight, studied by SEM, and compared with the fresh non-wovens.

For fluorescence microscopy, pure PCL fibers containing 5.0% FITC-labeled lysozyme crystals were electrospun onto cover slits. Electrospinning conditions were the same as those for 10.1 μm pure PCL fibers. Fluorescence images were recorded using an Axio Observer Z1 epifluorescence microscope (Zeiss, Oberkochen, Germany) with excitation at 450−490 nm (λ), a beam splitter at 495 nm (λ), and emission at 500−550 nm (λ) using a Plan-Apochromat 63×/1.40 objective and an AxioCam MRm camera.

2.8. Wettability of the Non-Wovens. Direct measurement of the contact angle using sessile drop goniometry is difficult for non-wovens because of the rough surface and high capillarity. Consequently, we determined the sorption rate of release buffer to characterize the wettability of the non-wovens using a tensiometer (K12, Krüss GmbH, Hamburg, Germany). The non-wovens were cut into pieces of equal size (9 mm × 18 mm) and connected to the balance of the tensiometer. The short side of the sample was immersed exactly 0.5 mm into the release buffer (PBS with 0.1% sodium azide). The mass increase was recorded over 10 min, and the squared mass was plotted versus time. The Washburn theory describes the relationship between the time and the adsorbed mass of liquid as follows.[23,24]

$$t = Am^2 \tag{1}$$

$$A = \frac{\eta}{c\rho^2\sigma \times \cos\theta} \tag{2}$$

where m is the sorbed mass of water, η is the viscosity of the immersion liquid, c is the capillarity of the sample, ρ is the density of the immersion liquid, σ is the surface tension of the immersion liquid, and θ is the contact angle between the immersion liquid and non-woven. Assuming similar capillarity, the sorbed mass of water directly correlates with the contact

angle between the liquid and non-woven and, therefore, represents a simple measure for assessing the wettability of non-wovens.

2.9. Statistical Analysis. All data are reported as means ± the standard deviation of at least three independent experiments unless specified otherwise. Statistical significance was calculated with a Student's *t* test for comparison of two groups or one-way analysis of variance using multiple comparisons versus control by the Holm−Sidak method for comparison of multiple groups with an overall significance level of 0.05 (SigmaPlot 12, Systat Software, San Jose, CA).

3. RESULTS

3.1. Morphology of Lysozyme Crystals and Non-Wovens. Lysozyme crystals were produced at a yield of approximately 92%, achieving narrow size distributions and minimal aggregation (Figure S1 of the Supporting Information). Two different crystals with diameters of 0.7 ± 0.1 and 2.1 ± 0.7 μm were used in this study (Figure 1A,B). The purity of the resulting crystal powder was determined to be 85.9% for the 0.7 μm crystals and 85.6% for the 2.1 μm crystals. The relative biological activity was fully retained after incubation in the solvents used for electrospinning.

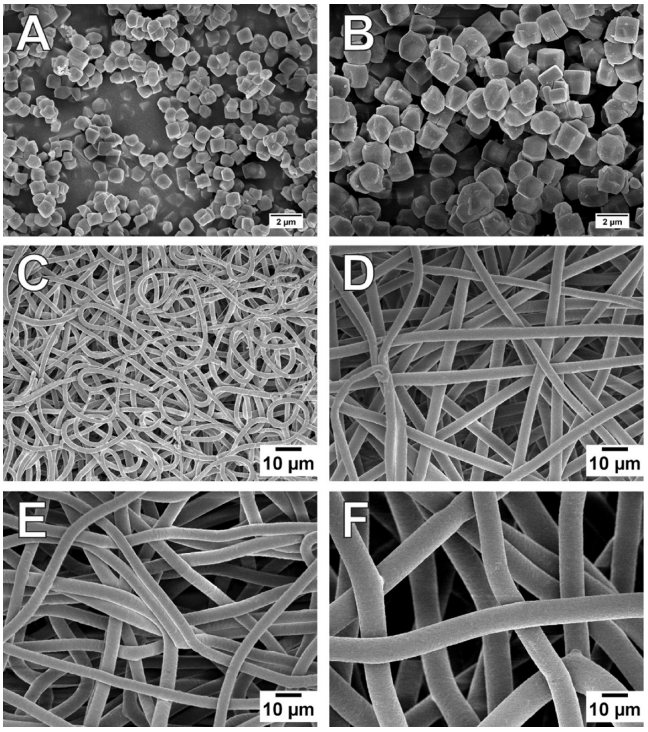

Figure 1. Scanning electron micrographs detailing the morphology of lysozyme crystals (A and B) and electrospun non-wovens (C−F). Lysozyme crystals approximately 0.7 μm (A) and 2.1 μm (B) in average diameter were used in this study. Non-wovens were generated by electrospinning from PCL solutions in a chloroform/ethanol mixture containing suspended lysozyme crystals. Average fiber diameters were approximately 1.6 (C), 3.6 (D), 5.2 (E), and 10.2 μm (F).

The fiber diameter, shape, and surface were examined using SEM. It is to be noted that single lysozyme crystals were not observed outside a fiber. Electrospinning of pure PCL was highly reproducible, allowing the repeated production of non-wovens with narrow fiber size distributions (Table 1 and Figure S2A of the Supporting Information). The surface of the fibers appeared to be smooth, and no pores were observed (Figure 1C−F).

Electrospinning process parameters had to be adapted for PCL/PEG blends as compared to the protocol used for PCL to account for the decreased viscosity of the solution (Table 2). Nevertheless, a statistically significant decrease in fiber diameter from 6.8 ± 1.1 μm for blends containing 2% PEG to 5.6 ± 1.1 μm for the 20% PEG blend was observed. However, the high degree of uniformity of fiber diameters was not compromised under the modified conditions (Figure S2B of the Supporting Information). The addition of PEG resulted in the formation of pores or depressions on the surface, whose size increased with increasing PEG content (Figure 2A−C). At 20% PEG, the fiber morphology changed to a coarse, wrinkled surface with no distinct pores (Figure 2D).

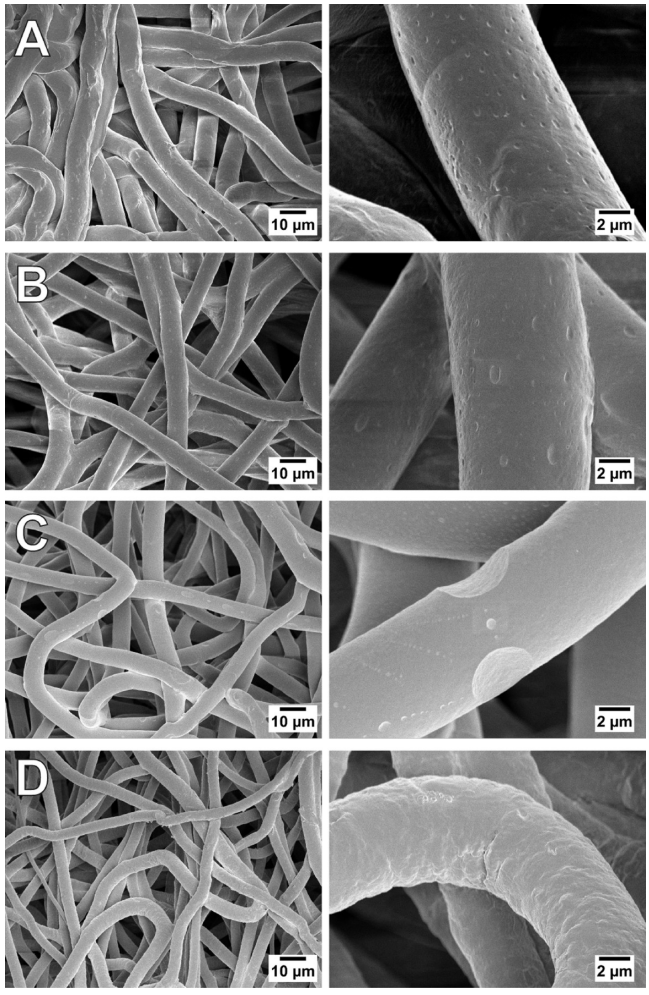

Figure 2. Scanning electron micrographs of PCL/PEG blend non-wovens at 2% (A), 5% (B), 10% (C), and 20% PEG (D) at low (left) and high (right) magnifications.

The PCL/PLGA spinning process was less stable than PCL or PCL/PEG spinning, resulting in an increasing relative standard deviation of fiber diameters from 9.8% for pure PCL fibers to 34.8% in the case of 2% PLGA and 53.5% for 10% PLGA fibers (Figure S2C of the Supporting Information). Again, with an increasing PLGA content, a statistically significant decrease in fiber diameter from 9.9 ± 3.4 to 8.2 ±

dx.doi.org/10.1021/mp5001026 | *Mol. Pharmaceutics* 2014, 11, 2372−2380

4.4 μm and an increase in surface roughness were observed (Figure 3A,B). PCL/PLGA blends with a PLGA content of

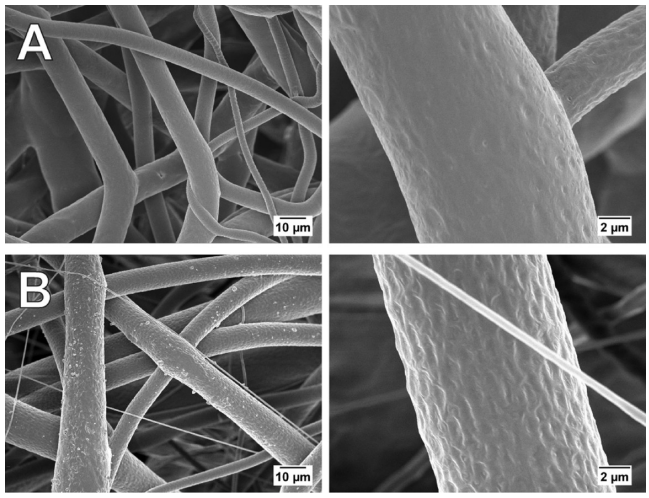

Figure 3. Scanning electron micrographs of PCL/PLGA blend non-wovens at 2% (A) and 10% PLGA (B) at low (left) and high (right) magnifications.

>10% resulted in reduced viscosity and phase separation and thus were not suitable for electrospinning. During release, no change in fiber morphology was detected by SEM in the case of PCL/PEG scaffolds, while minimal shrinking and formation of few large pores were observed in the case of PCL/PLGA non-wovens (Figure S3 of the Supporting Information).

Using fluorescence microscopy, it was confirmed that crystals kept their shape after being incorporated into electrospun fibers and that all crystals were located within the fibers (Figure 4).

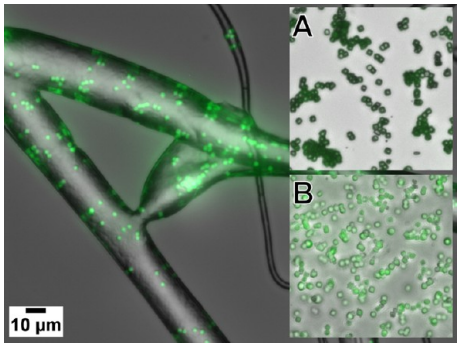

Figure 4. Distribution of FITC-labeled lysozyme crystals in a PCL non-woven prepared using 2.1 μm lysozyme crystals, a 25% PCL solution, and a drug loading of 5%. Inset A shows unprocessed lysozyme crystals suspended in air, while inset B shows lysozyme crystals embedded in a film cast from the same crystal suspension in a PCL solution used for electrospinning of the fibers. The scale bar applies to the main image and the insets.

Crystals were evenly and discretely distributed within individual fibers and could be observed within the entire non-woven. The distance to the fiber surface appeared to be irregular. The effect of processing on the morphology and distribution of lysozyme crystals was evaluated in detail by comparing unprocessed lysozyme crystals suspended in air (Figure 4, inset A) to crystals in PCL cast as a film using the same lysozyme crystal/PCL suspension that was used for electrospinning (Figure 4, inset B). The size and morphology of lysozyme crystals after suspension in PCL in a chloroform/ethanol mixture and film casting were unchanged compared to those of unprocessed lysozyme crystals. Lysozyme crystals in electrospun fibers had the same morphology but appeared to be slightly smaller than those in cast films, which may be explained by the curvature of fibers resulting an optically reduced size of particles within the fiber.

3.2. Effect of Scaffold Composition on Lysozyme Release, Relative Bioactivity, and Sorption of Release Buffer. The release of lysozyme from PCL fibers depended on fiber diameter as well as on the size of the protein crystals. The burst release was efficiently controlled by both parameters (Figure 5A,B). For both 0.7 and 2.1 μm lysozyme crystals, a statistically significant inverse relation of burst release to fiber diameter was observed (Figure 5C). Furthermore, burst release from fibers with a similar diameter was consistently and statistically significantly higher for larger protein crystals (Figure 5C). Interestingly, this was confirmed even for the combination of 2.1 μm crystals with 1.5 μm fibers, potentially because of the coating of the crystals with a thin PCL film controlling the release. Using pure PCL as a scaffold material, only the amount of burst differed; the subsequent release was in all cases minimal and was not affected by fiber diameter or crystal size (Figure 5A,B).

The effect of lysozyme loading under otherwise identical conditions was varied to delineate the drug loading potential of the delivery system as well as the effect of loading on drug release (Figure 6). Processability was not affected within the chosen loading range. Interestingly, for drug loading between 0.5 and 5%, no effect of loading on relative lysozyme release was observed (Figure 6A). Absolute drug release is shown in Figure 6B, confirming that the amount of lysozyme released could be directly controlled by the loading. A linear relationship between the absolute amount of lysozyme released after 24 h and drug loading was found (Figure 6C; R^2 = 0.982).

PEG was added to the system in different ratios as a pore-forming agent and to improve wettability of non-wovens compared to that of pure PCL as described previously[9,10] and as confirmed by sorption experiments (see below). Addition of up to 10% PEG had no significant effect on the release pattern compared to the effect of pure PCL (Figure 7A). At 20% PEG, a significant increase in the level of released lysozyme was found for the first 21 days, followed by minimal release thereafter (Figure 7A).

Therefore, PCL/PLGA blends were used to further improve the release by increasing the level of polymer degradation (Figure 7B). After addition of 10% PLGA, a burst of around 5% of total encapsulated lysozyme was observed, which was significantly higher than the burst from pure PCL scaffolds under otherwise comparable conditions. Thereafter, lysozyme was released at an almost constant rate for ~5 weeks. However, lysozyme degradation products were detected by RP-HPLC after ~1 week (Figure S4 of the Supporting Information). After 5 weeks, no further increase in the magnitude of the lysozyme main peak was observed in the release medium, and the pH value of the release buffer decreased to 3.3, most likely because of acidic PLGA degradation products. As exchange of the release medium was minimal (approximately 7% of the medium was exchanged per time point), the decrease in pH led to degradation of already released lysozyme, resulting in a decreasing cumulative lysozyme concentration after incubation for 5 weeks. At 2% PLGA, the level of lysozyme degradation was significantly reduced and an almost constant release rate

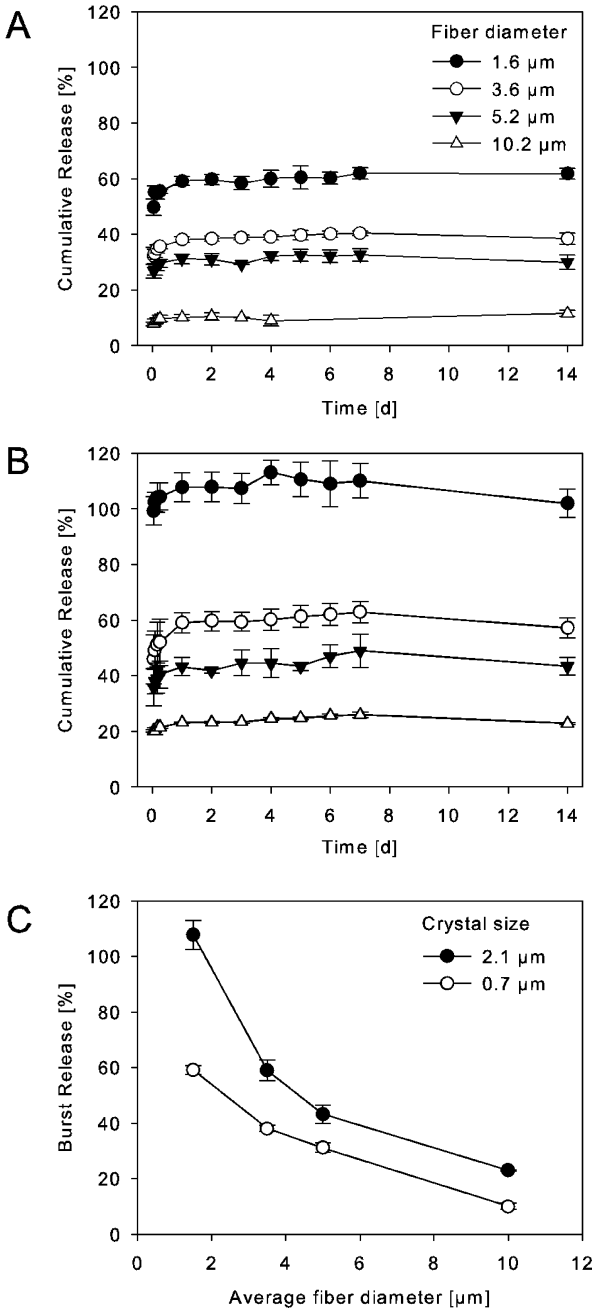

Figure 5. Release of lysozyme from pure PCL non-wovens with average fiber diameters of 1.6, 3.6, 5.2, and 10.2 μm using approximately 0.7 μm (A) and 2.1 μm (B) lysozyme crystals. (C) Relationship among fiber diameter, crystal size, and burst release. The averages and standard deviations of three independent experiments are shown.

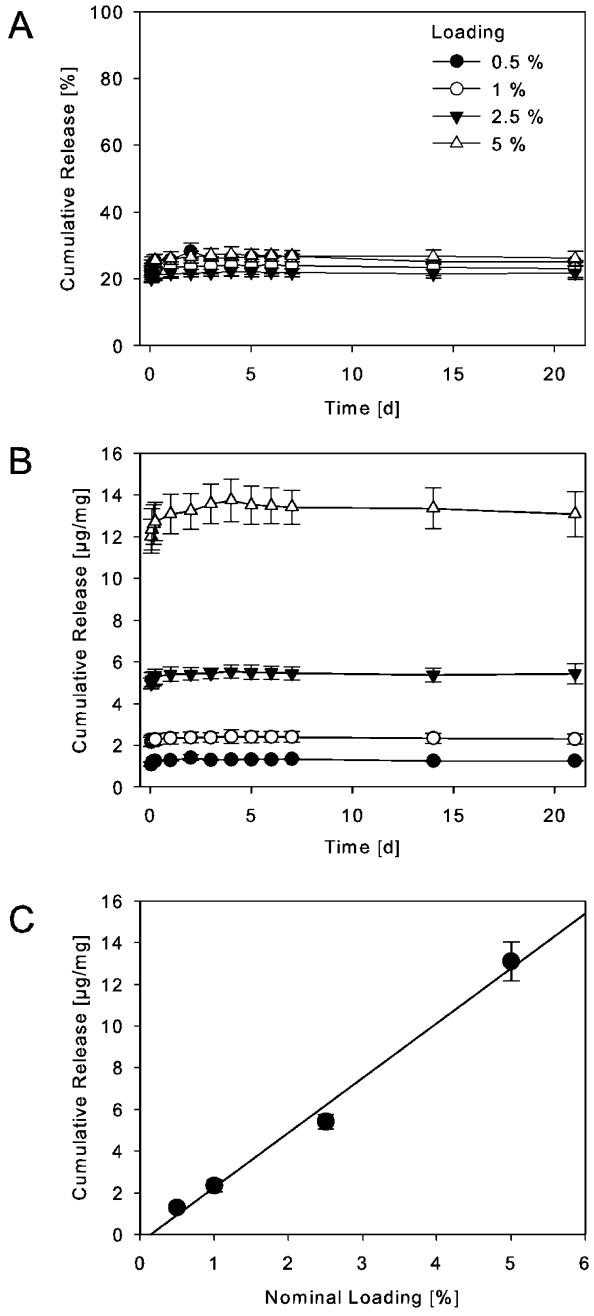

Figure 6. Effect of variation of lysozyme loading on the release from pure PCL non-wovens with an average fiber diameter of 7.1 μm and using approximately 2.1 μm lysozyme crystals. Cumulative relative release (A) and cumulative absolute release (B) of lysozyme. A linear relationship between loading and burst release was observed (C). The averages and standard deviations of three independent experiments are shown.

was observed for 11 weeks. Under these conditions, the pH decreased to 5.2 within 11 weeks. For both PCL/PLGA blends, the level of lysozyme release was statistically significantly higher than the level of release from pure PCL scaffolds.

The relative bioactivity of samples taken at the end of the release study was determined and related to the content determined by RP-HPLC. Lysozyme released from pure PCL or PCL/PEG scaffolds showed no decrease in relative bioactivity after 3 weeks. The relative bioactivity of lysozyme released from PCL/PLGA scaffolds after 11 weeks was 84.5 ± 1.8% in the case of 2% PCL/PLGA blends, whereas the relative bioactivity in the case of 10% PCL/PLGA blends was significantly lower (67.0 ± 8.3%).

Sorption measurements were performed to assess the wettability of the scaffolds (Figure 8). In contrast to classic wicking experiments, the rate of buffer sorption was determined per area of the non-woven in contact with the solution but the contact angle was not calculated because of the unknown scaffold porosity. Pure PCL non-wovens showed the least sorption with only little buffer uptake during the experiment. As expected, the addition of polysorbate 80 to the release medium

dx.doi.org/10.1021/mp5001026 | Mol. Pharmaceutics 2014, 11, 2372−2380

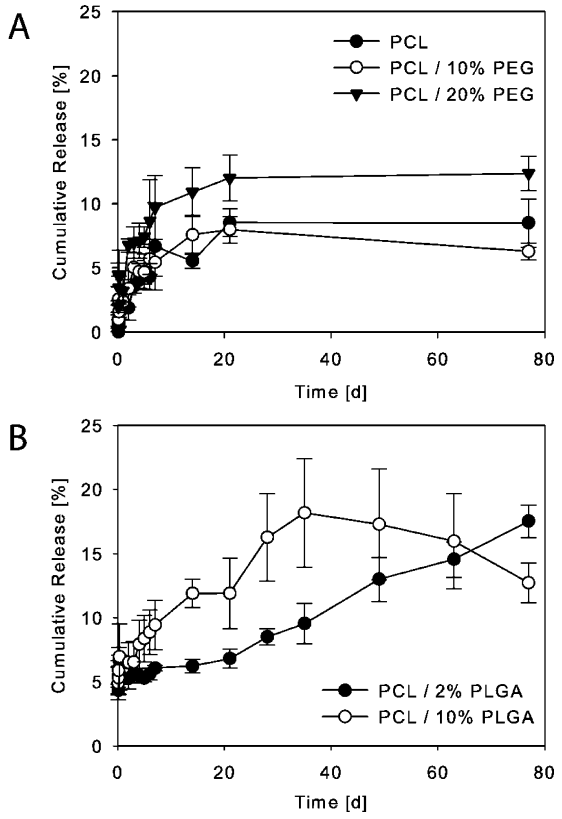

Figure 7. Release of lysozyme from PCL/PEG and PCL/PLGA scaffolds at a constant fiber diameter and crystal size. The effect of addition of increasing amounts of PEG (A) and PLGA (B) relative to pure PCL is shown. Results are presented as averages and standard deviations of three independent experiments.

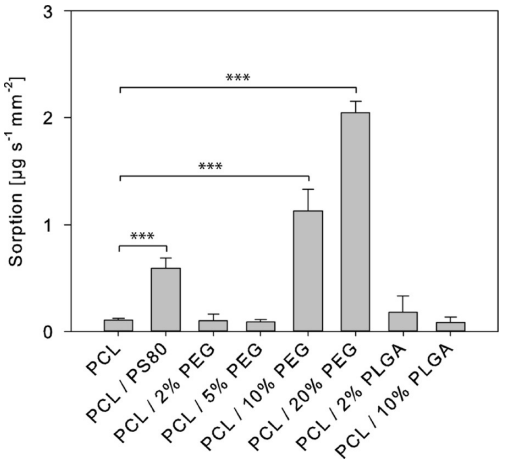

Figure 8. Dependence of sorption of release buffer by electrospun non-wovens on polymer composition and addition of surfactant. The averages and standard deviations of three independent experiments are shown.

resulted in a statistically significantly increased level of sorption, i.e., improved wetting of scaffolds. Addition of 10 and 20% PEG but not of 2 or 5% PEG resulted in a significantly increased level of sorption. In contrast, the wettability of PCL/PLGA blends was not significantly increased compared to that of pure PCL scaffolds.

4. DISCUSSION

The application of protein crystals is an emerging strategy for addressing several problems related to the processing, storage, and delivery of biologic drugs.[15,25−28] Notably, protein crystals possess higher thermodynamic stability, smaller contact surface area, and higher purity than the amorphous state.[12,29] The control of crystallization conditions allows the generation of particles of varying size and with almost monomodal size distribution (Figure 1A,B).[17] Furthermore, the crystalline state opens new avenues for the development of electrospun protein delivery systems, from a processing perspective as well as with regard to the control of release profiles. Organic solvents that otherwise would lead to denaturation of the protein can be used during electrospinning of protein crystal suspensions.[15] Of course, solvents must be carefully selected such that protein crystals neither dissolve nor unfold or aggregate during processing. Lysozyme crystals could be dispersed in a mixture of chloroform and ethanol without a detectable loss of relative biological activity. After incorporation of lysozyme crystals into electrospun scaffolds composed of PCL and PCL/PEG or PCL/PLGA blends, the lysozyme crystal integrity and overall morphology were retained. Sedimentation during the electrospinning operation was successfully prevented by high viscosities of concentrated polymer solutions, resulting in a homogeneous lysozyme crystal distribution within the scaffolds (Figure 4). The release of protein from non-woven scaffolds is often characterized by significant burst release at early time points, of which the extent is in many cases related to the conditions of scaffold preparation or scaffold composition.[30,31] However, control of burst release is rarely considered a design feature of a drug delivery system despite the fact that the release of a defined loading dose would in many cases be desirable from a pharmacokinetic perspective.[32,33] As shown herein, burst release can be modified in a manner independent of the subsequent release rate by means of a rational combination of lysozyme crystal size and PCL fiber diameter (Figure 5), therefore opening new options for controlled protein delivery. We hypothesize that the variable burst release can be explained primarily using geometrical considerations. For a constant fiber diameter, the likelihood that parts of a protein crystal are located at or very close to the fiber surface positively correlates with crystal size, and therefore, the level of burst release increases with an increasing ratio of crystal size to fiber diameter. By SEM, no crystals or parts of crystals exposed at the fiber surface were found (Figure 1). We therefore assume that burst release originates from lysozyme crystals that are very close to the surface and are covered only with a thin PCL film, allowing fast diffusion of water and dissolved lysozyme. An interesting feature of a drug delivery system composed of protein crystals embedded in non-woven polymer fibers is the ability to vary drug loading within broad margins without affecting relative drug release (Figure 6A−C). Absolute protein release can therefore be directly defined by variation of drug loading. Subsequent lysozyme release was negligible in all cases because of the fact that PCL degradation under *in vitro* release conditions is very slow in general and further reduced in the case of non-woven scaffolds.[34] Apart from release driven by polymer degradation, solid state diffusion and desorption of encapsulated drugs from nanopores may contribute to the release of protein from PCL scaffolds.[30,35] A classic approach to further improve release under such circumstances is to increase the porosity of the scaffolds by blending with, e.g., low-

molecular weight PEG.[11] Furthermore, the wettability of PCL/PEG fibers is significantly improved compared to that of pure PCL by addition of PEG (Figure 8). However, up to 10% PEG content, the release profiles were comparable to those of pure PCL fibers. Increasing the PEG content to 20% changed the fiber morphology and resulted in increased release rates within the first 3 weeks (Figures 2D and 7A). In contrast to our findings, a pronounced effect of addition of PEG to PCL fibers containing dissolved/amorphous lysozyme on release rate was found by Li et al., highlighting the profound differences between a drug delivery system within which a molecular dispersion of drug is used and a system representing a coarse drug suspension in a polymer matrix.[10]

Finally, PCL/PLGA blends were employed to tailor the release rate. In contrast to simple pore formation as in the case of PEG, the combination of PLGA and PCL was selected to improve release because of the following three effects. First, the PLGA degradation rate is much higher than that of PCL, resulting in an increased overall degradation rate of the polymer blend. Second, PLGA degradation results in the local release of acidic degradation products that may catalyze and hence increase the level of PCL ester hydrolysis.[36] Third, in contrast to PCL, PLGA is known to show significant swelling during release, potentially resulting in weakening of the scaffold structure with improved penetration of the release medium.[37] Water sorption was not affected by the addition of PLGA compared to pure PCL scaffolds (Figure 8). Consequently, improved release as a result of increased wettability of the scaffolds may be excluded. Both PLGA blends showed an increased burst effect compared to pure PCL and significantly increased release rates (Figure 7B). The level of lysozyme degradation was increased during release from PCL/PLGA scaffolds and positively correlated with PLGA content. PLGA degradation is known to negatively affect protein integrity and stability because of the generation of acidic degradation products.[38] The *in vitro* release setup chosen herein resulting in minimal exchange of release medium at each sampling time point exaggerates the detrimental effects of PLGA degradation. In an *in vivo* setting, a higher fluid exchange rate and, therefore, a reduced level of protein degradation may be assumed. Nevertheless, the PLGA content must be carefully balanced to achieve an appropriate release rate while reducing the level of protein degradation. Despite the improved release of lysozyme from PCL/PLGA compared to pure PCL non-wovens, the morphology remained largely unchanged throughout the release except for pore formation (Figure S4 of the Supporting Information).

In summary, our results could pave the way to the controlled release of crystalline proteins embedded in electrospun non-wovens. We have provided evidence that the burst release, wettability, and release rate can be tailored, allowing the specific requirements in various applications of protein-loaded non-wovens to be fulfilled.

5. CONCLUSIONS

Incorporating crystallized proteins into non-wovens offers numerous possibilities for the delivery of peptides and proteins. Relevant fields of application of non-wovens for controlled protein delivery are the treatment of dermal wounds and localized drug release after surgical interventions, e.g., after tumor excision. We show that protein crystals can successfully be embedded into electrospun non-wovens while preserving protein relative bioactivity. The burst effect could be controlled by a rational combination of fiber diameter, crystal size, and loading. Release rates following burst from pure PCL scaffolds were constant and independent of crystal size, fiber diameter, and loading. The wettability of non-wovens was controlled by addition of a hydrophilic porogen to the PCL matrix, and the release rate was increased at PEG concentrations of 20%. Admixing PLGA to PCL resulted in non-wovens with a tunable release rate achieving an almost linear release over 11 weeks under optimized conditions.

■ ASSOCIATED CONTENT

Supporting Information

Detailed information about the HPLC solvent gradient, particle size distribution of lysozyme crystals, fiber diameter distributions after electrospinning of different polymer formulations, morphology of PCL/PEG non-wovens, and lysozyme degradation. This material is available free of charge via the Internet at http://pubs.acs.org.

■ AUTHOR INFORMATION

Corresponding Author

*Institute of Pharma Technology, University of Applied Sciences Northwestern Switzerland, Gruendenstrasse 40, CH-4132 Muttenz, Switzerland. E-mail: oliver.germershaus@fhnw.ch.

Notes

The authors declare no competing financial interest.

■ REFERENCES

(1) Formhals, A. Apparatus for Producing Artificial Filaments from Material such as Cellulose Acetate. 1934. U.S. patent 1,975,504.

(2) Formhals, A. Method and apparatus for spinning. 1937. U.S. patent 2,349,950.

(3) Meinel, A. J.; Germershaus, O.; Luhmann, T.; Merkle, H. P.; Meinel, L. Electrospun matrices for localized drug delivery: Current technologies and selected biomedical applications. *Eur. J. Pharm. Biopharm.* **2012**, *81* (1), 1−13.

(4) Dash, T. K.; Konkimalla, V. B. Poly-ε-caprolactone based formulations for drug delivery and tissue engineering: A review. *J. Controlled Release* **2012**, *158* (1), 15−33.

(5) Cipitria, A.; Skelton, A.; Dargaville, T. R.; Dalton, P. D.; Hutmacher, D. W. Design, fabrication and characterization of PCL electrospun scaffolds: A review. *J. Mater. Chem.* **2011**, *21* (26), 9419−9453.

(6) Chen, D. R.; Bei, J. Z.; Wang, S. G. Polycaprolactone microparticles and their biodegradation. *Polym. Degrad. Stab.* **2000**, *67* (3), 455−459.

(7) Zong, X. H.; Li, S.; Chen, E.; Garlick, B.; Kim, K. S.; Fang, D. F.; Chiu, J.; Zimmerman, T.; Brathwaite, C.; Hsiao, B. S.; Chu, B. Prevention of postsurgery-induced abdominal adhesions by electrospun bioabsorbable nanofibrous poly(lactide-co-glycolide)-based membranes. *Ann. Surg.* **2004**, *240* (5), 910−915.

(8) Cao, X. D.; Shoichet, M. S. Delivering neuroactive molecules from biodegradable microspheres for application in central nervous system disorders. *Biomaterials* **1999**, *20* (4), 329−339.

(9) Maretschek, S.; Greiner, A.; Kissel, T. Electrospun biodegradable nanofiber nonwovens for controlled release of proteins. *J. Controlled Release* **2008**, *127* (2), 180−187.

(10) Li, Y.; Jiang, H. L.; Zhu, K. J. Encapsulation and controlled release of lysozyme from electrospun poly(ε-caprolactone)/poly(ethylene glycol) non-woven membranes by formation of lysozyme-oleate complexes. *J. Mater. Sci.: Mater. Med.* **2008**, *19* (2), 827−832.

(11) Lu, C. H.; Lin, W. J. Permeation of protein from porous poly(ε-caprolactone) films. *J. Biomed. Mater. Res.* **2002**, *63* (2), 220−225.

(12) Shenoy, B.; Wang, Y.; Shan, W. Z.; Margolin, A. L. Stability of crystalline proteins. *Biotechnol. Bioeng.* **2001**, *73* (5), 358−369.

(13) Yang, M. X.; Shenoy, B.; Disttler, M.; Patel, R.; McGrath, M.; Pechenov, S.; Margolin, A. L. Crystalline monoclonal antibodies for subcutaneous delivery. *Proc. Natl. Acad. Sci. U.S.A.* **2003**, *100* (12), 6934−6939.
(14) Elkordy, A. A.; Forbes, R. T.; Barry, B. W. Integrity of crystalline lysozyme exceeds that of a spray-dried form. *Int. J. Pharm.* **2002**, *247* (1−2), 79−90.
(15) Pechenov, S.; Shenoy, B.; Yang, M. X.; Basu, S. K.; Margolin, A. L. Injectable controlled release formulations incorporating protein crystals. *J. Controlled Release* **2004**, *96* (1), 149−158.
(16) Muller, C.; Ulrich, J. The dissolution phenomenon of lysozyme crystals. *Cryst. Res. Technol.* **2012**, *47* (2), 169−174.
(17) Falkner, J. C.; Al-Somali, A. M.; Jamison, J. A.; Zhang, J. Y.; Adrianse, S. L.; Simpson, R. L.; Calabretta, M. K.; Radding, W.; Phillips, G. N.; Colvin, V. L. Generation of size-controlled, submicrometer protein crystals. *Chem. Mater.* **2005**, *17* (10), 2679−2686.
(18) Bueno, V. B.; Petri, D. F. Xanthan hydrogel films: Molecular conformation, charge density and protein carriers. *Carbohydr. Polym.* **2014**, *101*, 897−904.
(19) Charernsriwilaiwat, N.; Opanasopit, P.; Rojanarata, T.; Ngawhirunpat, T. Lysozyme-loaded, electrospun chitosan-based nanofiber mats for wound healing. *Int. J. Pharm.* **2012**, *427* (2), 379−384.
(20) Nakatsuji, T.; Gallo, R. L. Antimicrobial peptides: Old molecules with new ideas. *J. Invest. Dermatol.* **2012**, *132* (3, Part 2), 887−895.
(21) Pham, Q. P.; Sharma, U.; Mikos, A. G. Electrospun poly(ε-caprolactone) microfiber and multilayer nanofiber/microfiber scaffolds: Characterization of scaffolds and measurement of cellular infiltration. *Biomacromolecules* **2006**, *7* (10), 2796−2805.
(22) Liao, Y. H.; Brown, M. B.; Martin, G. P. Turbidimetric and HPLC assays for the determination of formulated lysozyme activity. *J. Pharm. Pharmacol.* **2001**, *53* (4), 549−554.
(23) Washburn, E. W. Note on a Method of Determining the Distribution of Pore Sizes in a Porous Material. *Proc. Natl. Acad. Sci. U.S.A.* **1921**, *7* (4), 115−116.
(24) Washburn, E. W. The dynamics of capillary flow. *Phys. Rev.* **1921**, *17*, 273−283.
(25) Zang, Y. G.; Kammerer, B.; Eisenkolb, M.; Lohr, K.; Kiefer, H. Towards Protein Crystallization as a Process Step in Downstream Processing of Therapeutic Antibodies: Screening and Optimization at Microbatch Scale. *PLoS One* **2011**, *6* (9), e25282.
(26) Hebel, D.; Huber, S.; Stanislawski, B.; Hekmat, D. Stirred batch crystallization of a therapeutic antibody fragment. *J. Biotechnol.* **2013**, *166* (4), 206−211.
(27) Miller, M. A.; Engstrom, J. D.; Ludher, B. S.; Johnston, K. P. Low Viscosity Highly Concentrated Injectable Nonaqueous Suspensions of Lysozyme Microparticles. *Langmuir* **2010**, *26* (2), 1067−1074.
(28) Govardhan, C.; Khalaf, N.; Jung, C. W.; Simeone, B.; Higbie, A.; Qu, S.; Chemmalil, L.; Pechenov, S.; Basu, S. K.; Margolin, A. L. Novel long-acting crystal formulation of human growth hormone. *Pharm. Res.* **2005**, *22* (9), 1461−1470.
(29) Elkordy, A. A.; Forbes, R. T.; Barry, B. W. Stability of crystallised and spray-dried lysozyme. *Int. J. Pharm.* **2004**, *278* (2), 209−219.
(30) Gandhi, M.; Srikar, R.; Yarin, A. L.; Megaridis, C. M.; Gemeinhart, R. A. Mechanistic Examination of Protein Release from Polymer Nanofibers. *Mol. Pharmaceutics* **2009**, *6* (2), 641−647.
(31) Williamson, M. R.; Chang, H. I.; Coombes, A. G. A. Gravity spun polycaprolactone fibres: Controlling release of a hydrophilic macromolecule (ovalbumin) and a lipophilic drug (progesterone). *Biomaterials* **2004**, *25* (20), 5053−5060.
(32) Finkelstein, A.; McClean, D.; Kar, S.; Takizawa, K.; Varghese, K.; Baek, N.; Park, K.; Fishbein, M. C.; Makkar, R.; Litvack, F.; Eigler, N. L. Local drug delivery via a coronary stent with programmable release pharmacokinetics. *Circulation* **2003**, *107* (5), 777−784.
(33) Zeng, J.; Aigner, A.; Czubayko, F.; Kissel, T.; Wendorff, J. H.; Greiner, A. Poly(vinyl alcohol) nanofibers by electrospinning as a protein delivery system and the retardation of enzyme release by additional polymer coatings. *Biomacromolecules* **2005**, *6* (3), 1484−1488.
(34) Bolgen, N.; Menceloglu, Y. Z.; Acatay, K.; Vargel, I.; Piskin, E. In vitro and in vivo degradation of non-woven materials made of poly(ε-caprolactone) nanofibers prepared by electrospinning under different conditions. *J. Biomater. Sci., Polym. Ed.* **2005**, *16* (12), 1537−1555.
(35) Srikar, R.; Yarin, A. L.; Megaridis, C. M.; Bazilevsky, A. V.; Kelley, E. Desorption-limited mechanism of release from polymer nanofibers. *Langmuir* **2008**, *24* (3), 965−974.
(36) Siparsky, G. L.; Voorhees, K. J.; Miao, F. D. Hydrolysis of polylactic acid (PLA) and polycaprolactone (PCL) in aqueous acetonitrile solutions: Autocatalysis. *J. Environ. Polym. Degrad.* **1998**, *6* (1), 31−41.
(37) Anderson, J. M.; Shive, M. S. Biodegradation and biocompatibility of PLA and PLGA microspheres. *Adv. Drug Delivery Rev.* **1997**, *28* (1), 5−24.
(38) Crotts, G.; Park, T. G. Protein delivery from poly(lactic-co-glycolic acid) biodegradable microspheres: Release kinetics and stability issues. *J. Microencapsulation* **1998**, *15* (6), 699−713.